Taxol-Loaded Nanoparticles with Methoxy Poly(ethylene glycol)-*b*-Poly(ε-caprolactone) as a Novel Additive in the Outer Aqueous Phase

Yanting Zhang, Jingwen Hou, Changyun Qian, Lei Song, Shengrong Guo

School of Pharmacy, Shanghai Jiao Tong University, Shanghai 200240, China

Received 24 February 2010; accepted 27 September 2010
DOI 10.1002/app.33518
Published online 21 March 2011 in Wiley Online Library (wileyonlinelibrary.com).

ABSTRACT: Taxol-loaded nanoparticles were prepared by solvent-evaporation technique with methoxy-added methoxy poly(ethylene glycol)-*b*-poly(ε-caprolactone) (MPEG-*b*-PCL) (PEG wt % = 18.5%) as drug carrier and MPEG-*b*-PCL (PEG wt % = 86.8%) as the additive in the outer aqueous phase. The MPEG-*b*-PCL copolymers were synthesized via ring-opening polymerization of ε-caprolactone using Novozym 435 as biocatalyst. As a newly used additive in the outer aqueous phase, only 0.1% (w/v) MPEG-*b*-PCL with relatively high-PEG content was needed. The effects of feed ratio of taxol to copolymer (w/w, 5–20%) on the characters of nanoparticles and *in vitro* drug release were investigated. The fabricated nanoparticles reached the highest encapsulation efficiency of 52.5% ± 3.9% when the feed ratio was 10%. The nanoparticles presented a core-shell structure in aqueous solution, and their hydrodynamic diameter ranged from 75 to 105 nm. Transmission electron microscopy and atomic force microscope investigations exhibited that the nanoparticles had fine spherical shape and narrow particle size distribution. The size of nanoparticles did not change distinctly after incubation in pH 7.4 phosphate-buffered solution (PBS) and pH 7.4 PBS with 10% fetal bovine serum at 37°C for 24 h. The nanoparticles with drug loading around 5% could achieve a sustained drug release for 7 days. © 2011 Wiley Periodicals, Inc. J Appl Polym Sci 121: 2386–2393, 2011

Key words: taxol; methoxy poly(ethylene glycol)-*b*-poly (ε-caprolactone); nanoparticles; additive in the outer aqueous phase

INTRODUCTION

Taxol (paclitaxel) is one excellent natural antineoplastic drug against a wide spectrum of cancers, including breast and ovarian cancers.[1,2] Taxol has extremely poor solubility in aqueous media. To improve its solubility, an adjuvant called Cremophor EL (50 : 50 ethanol-polyoxyethylated castor oil) has to be added in the taxol injection (Taxol®), which may cause serious side effects, such as hypersensitivity reactions, nephrotoxicity, neurotoxicity, and cardiotoxicity.[3–5] Many dosage forms, such as liposomes, microspheres, nanoparticles, and polymeric micelles, are thus investigated to overcome the problems caused by Cremophor EL.[6–9] Among them, nanoparticles of biocompatible and biodegradable polymers have shown significant advantages in enhancing therapeutic efficacy and reducing systemic side effects.[10–14]

Conventional biodegradable polymeric nanoparticles are rapidly removed from bloodstream by the macrophages of the mononuclear phagocyte system (MPS) after intravenous administration. This prevents their application in controlled drug delivery and drug targeting to tissues other than MPS. Nanoparticles covered with poly (ethylene glycol) (PEG), however, may evade MPS uptake, at least to some extent, which exhibit prolonged residence in blood.[15,16]

Polymeric nanoparticles are usually produced by solvent-evaporation technique. Many factors can affect the nature of nanoparticles obtained, such as the additive as emulsifier or stabilizer in the outer aqueous phase. One of the most commonly used additives is poly(vinyl alcohol) (PVA), which can adsorb on the surface of nanoparticles and not be easily washed out. This may cause trouble in the purification of the products and thus influence the properties of the formed nanoparticles.[17,18] Besides, PVA is nondegradable and cannot be used as excipient for intravenous administration. Therefore, it is important to study novel additives having excellent properties.[19,20]

Correspondence to: S. Guo (srguo@sjtu.edu.cn).
Yanting Zhang and Jingwen Hou contributed equally to this work.

Contract grant sponsor: Specialized Research Fund for the Doctoral Program of Higher Education of China; contract grant number: 20090073110087.
Contract grant sponsor: National Grand New Drug Program, China; contract grant number; contract grant number: 2009ZX09310-007.
Contract grant sponsor: National Comprehensive Technology Platforms for Innovative Drug R&D, China; contract grant number: 2009ZX09301-007.

Some novel types of additives in the outer aqueous phase, such as vitamin E TPGS (D-α-tocopheryl polyethylene glycol 1000 succinate) and phospholipids, have been investigated to prepare nanoparticles. The size of the vitamin E TPGS emulsified nanoparticles ranged from 300 to 800 nm,[21] while that of phospholipids emulsified nanoparticles ranged from 600 to 700 nm.[19] In general, the nanoparticles with diameters smaller than 200 nm can evade the reticuloendothelial system and display enhanced permeability and retention effects at solid tumor sites.[22]

poly (e-caprolactone) (PCL) is good biocompatible and biodegradable, which has been widely used for bioabsorbable suture and particulate drug-delivery systems.[23,24] In our study, the methoxy poly(ethylene glycol)-*b*-poly(ε-caprolactone) (MPEG-*b*-PCL) copolymers with different PEG contents were synthesized via ring-opening polymerization of ε-caprolactone (ε-CL) using lipase as a nontoxic biocatalyst. We tried to fabricate the taxol-loaded nanoparticles by using the MPEG-*b*-PCL copolymers with a low-PEG content as drug carrier and the MPEG-*b*-PCL copolymers with a high-PEG content as the additive in the outer aqueous phase. The fabricated nanoparticles were covered with PEG chains in water, and their hydrodynamic diameters ranged from 75 to 105 nm.

EXPERIMENTAL

Materials

ε-CL was obtained from Acros Organic, dried over calcium hydride (CaH_2), and distilled under vacuum just before use. MPEG (M_n = 5000) from Fluka was used as received. Taxol of 99.0% purity was kindly supplied by Yunnan Ziyun Biotechnology Co. (China). Novozym 435 (Immobilized lipases from *Candida antarctica*) was purchased from Novozymes and dried *in vacuo* at room temperature for 24 h. PVA was obtained from Sinopharm Chemical Reagent Co. (Shanghai, China). Methanol used as mobile phase in high-performance liquid chromatography (HPLC) was purchased from Shanghai Xingke Biochemistry Co. (China).

Lipase-catalyzed synthesis of MPEG-*b*-PCL

The amphiphilic diblock copolymers composed of MPEG and ε-CL were synthesized as described previously.[25] A predetermined amount of MPEG was introduced into a 100-mL round-bottomed two-necked flask with 60-mL dried toluene. Residual water in the solution was removed by azeotropic distillation, resulting in 20 mL of MPEG/toluene solution (monomer versus toluene = 1/2 v/v). Novozym 435 (10 wt % of monomers) and ε-CL were transferred into the flask. The flask was then closed with a rubber stopper and immersed into an oil bath at 70°C with stirring for a predetermined time. Reactions were terminated by adding excess cold dichloromethane and removing the enzyme by filtration. Then, the filtrate was concentrated under reduced pressure to obtain the crude copolymers. The copolymers were further purified by reprecipitation (dichloromethane as a good solvent and cold methanol as a poor solvent) and dried *in vacuo* at room temperature.

Preparation of taxol-loaded MPEG-*b*-PCL nanoparticles

Taxol-loaded methoxy poly(ethylene glycol)-*b*-poly (ε-caprolactone) (MPEG-*b*-PCL) nanoparticles were prepared by solvent-evaporation method. First, 100 mg MPEG-*b*-PCL-1 (PEG wt % = 18.5%) and taxol (5, 10, 15, or 20 mg) were added and dissolved in 8 mL of dichloromethane. The resulting organic solution was added to 80 mL of ultrapure water containing 0.1% (w/v) MPEG-*b*-PCL-2 (PEG wt % = 86.8%) or 2% PVA, which kept stirring for 1.5 h at 20°C and for another 3 h at 40°C. The stirring rate was 800 rpm. Afterward, the possible nonincorporated drug particles and large aggregates were separated by centrifugation at 5000 rpm for 20 min. The supernatant was ultracentrifugated at 50,000 rpm for 60 min at 4°C to obtain the nanoparticles (Optima L-80XP, Beckman Coulter), and the obtained nanoparticles were washed three times with ultrapure water. The final products were lyophilized for 48 h.

Characterization of copolymers

FTIR spectra of polymers were recorded on a Perkin–Elmer Paragon 1000 FTIR spectrophotometer using KBr pellet technique.

^{1}H-NMR measurements by using a Mercury plus 400 spectrometer were used to characterize the copolymers and blank nanoparticles. One weight percent sample solution in $CDCl_3$ with 0.03 v/v% tetramethylsilane as an internal standard or 0.5 wt % blank nanoparticle solution in D_2O was used for the measurements.

The gel permeation chromatography (GPC) analyses for the copolymers were performed at 40°C using a Waters HPLC system equipped with a model 1525 binary HPLC pump, a model 2414 refractive index detector, and a series of Styragel™ columns (HR3 and HR4). Tetrahydrofuran was used as an eluent at a flow rate of 1.0 mL/min. The GPC system was calibrated with polystyrene standards.

The solubility of copolymers was measured by adding an excess amount of copolymer sample in 5-mL doubly distilled water and stirring the copolymer aqueous system at 37°C in a water bath for 48 h, so that dissolution equilibrium was reached. The undissolved copolymer samples were separated by centrifugation, lyophilized, and weighed. The solubility data were obtained by weight subtraction.

Measurement of encapsulation efficiency

The taxol content of nanoparticles was determined in triplicate by HPLC, equipped with a variable wavelength detector (SPD-10ADVP, Shimadzu, Japan). Three milligrams of lyophilized nanoparticles were dissolved in 1 mL of dichloromethane. A nitrogen stream was introduced to evaporate the dichloromethane, and 10 mL of methanol/water (75/25, v/v) was then added. The solution was ultrasonicated for 20 s and then centrifuged for 10 min at 10,000 rpm. The supernatant was collected for HPLC analysis. HPLC analysis was carried out under the following condition: Diamonsil^{TM} C_{18} column (250 mm × 4.6 mm, 5 μm, Dikma Technologies, Beijing, China), wavelength fixed at 227 nm, and mobile phase composed of methanol and water (75/25, v/v). The linearity of the response was verified over the concentration range of 0.1–100 μg/mL ($r^2 = 0.999$).

Particle size and zeta potential

The hydrodynamic diameters of nanoparticles were measured by DLS technique, using a Malvern Instrument Zetasizer Nano-S with scattering angle of 173° and 632-nm red laser at 25°C. The zeta potential of nanoparticles was measured by Particle Size Analyzer (90 Plus Model, Brookhaven Instruments) at 25°C. All the analyses were run in triplicate.

Morphology of nanoparticles

Transmission electron microscopy (TEM, JEM-2010/INCA OXFORD) and atomic force microscope (AFM, Bio Scope, Veeco Instruments) were used to determine the morphology of nanoparticles. A drop of nanoparticles solution containing 1 wt % phosphotungstic acid was placed on copper grid and dried before measurement by TEM at an acceleration voltage of 200 kV. Sample for AFM measurement was prepared as given below: a drop of nanoparticles solution was placed on a freshly cleaved mica substrate and rapidly frozen by liquid nitrogen; the frozen solution on a mica wafer was lyophilized for 48 h to remove water.

Stability of nanoparticles

The stability of taxol-loaded MPEG-*b*-PCL nanoparticles in ultrapure water at 4°C, pH7.4 phosphate-buffered solution (PBS 7.4) or PBS 7.4 containing 10% (v/v) fetal bovine serum (FBS 7.4) at 37°C, was evaluated by measuring the particle size.

In vitro release of taxol

Four milligrams of taxol-loaded MPEG-*b*-PCL nanoparticles were dispersed in 26 mL of PBS 7.4 containing 1% (w/v) Tween 80 in a capped centrifuge tube. Tween 80 was used to increase the solubility of taxol in the release medium to make it under the sink condition and reduce the association of drug with the container surface. The tube was placed in a shaking incubator (100 rpm) at 37°C. At the predetermined time intervals (i.e., 1, 3, 5, 8, 16, 24, 48, 72, 96, 120, 144, and 168 h), the tube was taken out from the incubator, and then the solution in tube was ultracentrifuged at 60,000 rpm for 15 min to separate the nanoparticles. After 4 mL of supernatant was withdrawn and 4 mL of fresh release medium was added, the precipitated nanoparticles were redispersed in release medium by shaking the tube for continuous release studies. The withdrawn supernatant was analyzed by HPLC.

RESULTS AND DISCUSSION

Characterization of MPEG-*b*-PCL copolymers

Methoxy poly(ethylene glycol)-*b*-poly(ε-caprolactone) (MPEG-*b*-PCL) copolymers with different PEG contents were synthesized via ring-opening polymerization of ε-CL using Novozym 435 as biocatalyst and

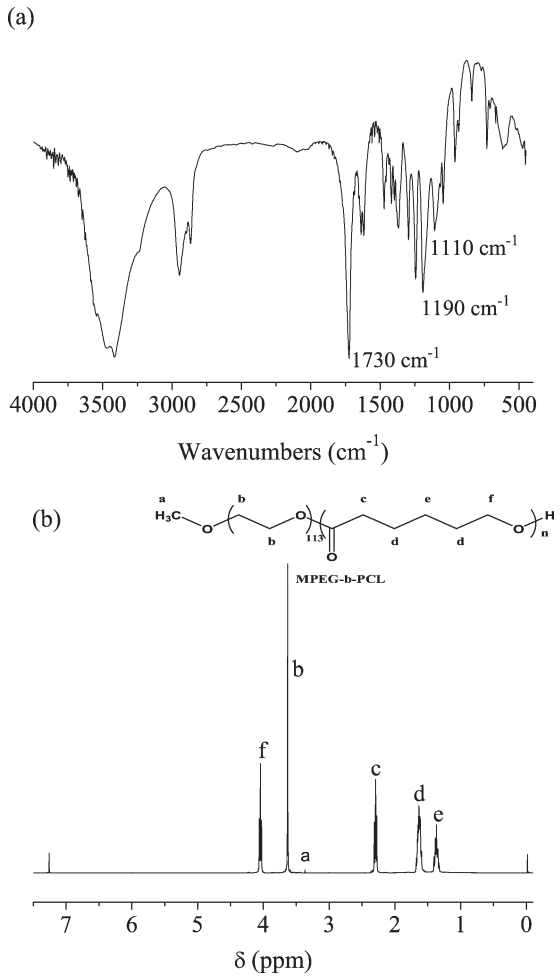

Figure 1 (a) FTIR spectrum of MPEG-*b*-PCL-1 copolymers; (b) ^{1}H-NMR spectrum of MPEG-*b*-PCL-1 copolymers in $CDCl_3$.

TABLE I
Characterization of MPEG-*b*-PCL Copolymers

Copolymers	PEG wt % in feed	PEG wt % in product[a]	M_{theo}[b]	M_{NMR}[a]	Polydispersity (M_w/M_n)[c]	Yield (%)	Water solubility (mg/mL)
MPEG-*b*-PCL-1	20	18.5	25,000	27,000	1.4	94	1.64 ± 0.10
MPEG-*b*-PCL-2	85	86.8	5,900	5,800	1.1	92	Gel formed at 365

[a] Calculated by ^{1}H-NMR.
[b] Calculated by the feed ratio.
[c] Determined by GPC.

MPEG as initiator. The structure of the resulting copolymers was confirmed by FTIR, ^{1}H-NMR, and GPC. The FTIR spectrum of MPEG-*b*-PCL-1 is shown in Figure 1(a). The peaks at 1730 and 1190 cm^{-1} were attributed to the C═O stretching vibration and C—O bonds of the ester group in PCL,[26] respectively. The peak at 1110 cm^{-1} was assigned to symmetric stretching vibration of C—O—C bonds in PEG.[27] Figure 1(b) shows the typical ^{1}H-NMR spectrum of MPEG-*b*-PCL-1 copolymer. The peaks at 3.65 ppm corresponded to protons at (b) in the PEG segments, and the peaks at 4.05 ppm were attributed to protons at f in the PCL segments. Based on the peak area ratio, the PEG wt % in copolymer was calculated.[28] The molecular weights calculated from NMR data (M_{NMR}) of the copolymers agreed well with the theoretical molecular weight based on the feed ratio (M_{theo}, see Table I). The copolymers showed unimodal GPC curves (data not shown). The polydispersity indices obtained from GPC analysis were small (see Table I), indicating narrow molecular weight distribution.

The solubility data of the copolymers are also listed in Table I. MPEG-*b*-PCL-1 with low-PEG contents had low solubility. However, MPEG-*b*-PCL-2 with high-PEG contents were highly water soluble. It was difficult to measure its solubility, because gel would form when the copolymer concentration was high.

Effect of the additive in the outer aqueous phase

The solvent-evaporation technique was applied in this study to fabricate nanoparticles. The additive in the outer aqueous phase plays a key role in the formation of uniform organic droplets and in the stabilization of the droplets during solvent evaporation. It also prevents the aggregation of the formed nanoparticles. As listed in Table II, when no additives were in the outer aqueous phase, no nanoparticles but only large aggregates could be obtained. We could obtain nanoparticles with small size when PVA or MPEG-*b*-PCL-2 was introduced as the additive in the outer aqueous phase. During the experiment, it was observed that the nanoparticles prepared using PVA as additive could not be completely dissolved in dichloromethane, which affected the measurements of drug contents and drug-encapsulation efficiency. It might be because that PVA could not be completely washed out of the nanoparticles and PVA was poorly soluble in dichloromethane. Unlike PVA, MPEG-*b*-PCL-2 was easily washed out. The nanoparticles prepared using MPEG-*b*-PCL-2 as additive were soluble in dichloromethane. Thus, we chose MPEG-*b*-PCL-2 as a novel additive to explore the properties of the taxol-loaded MPEG-*b*-PCL-1 nanoparticles. The chemical composition of the nanoparticles by using MPEG-*b*-PCL-1 as matrix material and MPEG-*b*-PCL-2 as the additive in the outer aqueous phase was analyzed by ^{1}H-NMR. The PEG wt % of the nanoparticles was 20.8%, almost the same as that of MPEG-*b*-PCL-1 (18.5%). It was suggested that the formed nanoparticles were only composed of MPEG-*b*-PCL-1, while MPEG-*b*-PCL-2 was not incorporated into the nanoparticles.

The core-shell structure of the nanoparticles was investigated by comparing the ^{1}H-NMR spectra of nanoparticles in $CDCl_3$ and in D_2O. The spectrum of blank nanoparticles in $CDCl_3$ was the same as that of MPEG-*b*-PCL-1 copolymer, in which the peaks of PEG and PCL blocks were all sharp and strong. But the peaks of PCL blocks, in the spectrum of the blank nanoparticles in D_2O (Fig. 2), became weak and broad while the peak of PEG blocks was still sharp and strong. These results indicated that the

TABLE II
Effects of Additives in the Outer Aqueous Phase on Nanoparticles

Additive in the outer aqueous phase	Hydrodynamic diameter (nm)[a]	Solubility of nanoparticles in dichloromethane
None	/	No nanoparticles were obtained
2% (w/v) PVA	101.3 ± 7.8	Not completely soluble
0.1% (w/v) MPEG-*b*-PCL-2	90.2 ± 2.6	Soluble

[a] Determined by DLS and expressed as average ± standard deviation ($n = 3$).

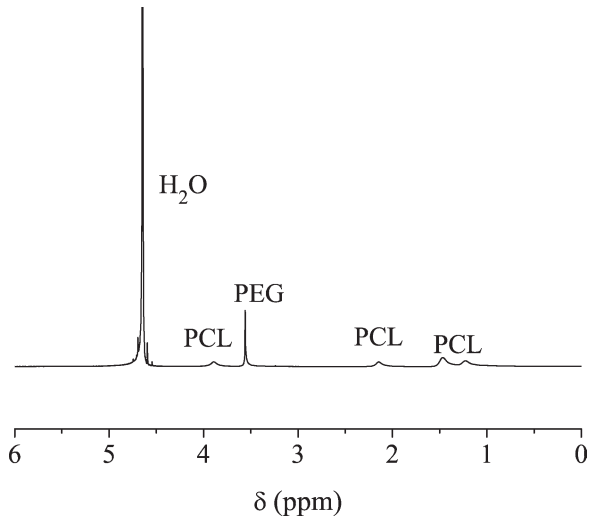

Figure 2 ^{1}H-NMR spectrum of blank MPEG-*b*-PCL-1 nanoparticles in D_2O.

PEG and PCL blocks were all fully dissolved in $CDCl_3$; however, in D_2O, PCL blocks were in a highly condensed state, and the PEG chains highly hydrated and extended away from the nanoparticle surface. It was suggested that the nanoparticles presented core-shell structure composed of condensed PCL cores and hydrated PEG shell in water.

Characterization of taxol-loaded MPEG-*b*-PCL nanoparticles

Encapsulation efficiency, particle size, and zeta potential

The encapsulation efficiency of taxol for the nanoparticles was measured. As shown in Table III, the encapsulation efficiency reached the maximum of 52.5% ± 3.9% when the drug content in feed was 10%. It was reported that 2% (w/v) PVA was needed to achieve the encapsulation efficiency of 40[19] or 50%,[29] while only 0.1% (w/v) MPEG-*b*-PCL-2 was needed to achieve the similar encapsulation efficiency in our study. This implied that MPEG-*b*-PCL-2 could be a more effective additive in the outer aqueous phase than traditional PVA.

The size and size distribution of the taxol-loaded nanoparticles were measured by DLS, and the data were tabulated in Table III. All samples had a narrow polydispersity within 0.150, and the mean hydrodynamic diameters ranged from 75 to 105 nm. The drug loading did not have significant effect on the nanoparticles size. It might be due to the low-drug loading (1.86–5.62%).

The zeta potential of the taxol-loaded nanoparticles was also characterized in order to determine the surface charge property. Zeta potential can be an important parameter for the stability of the nanoparticles.[30] In most circumstances, the higher the absolute value of the zeta potential of the nanoparticles, the larger the amount of charge on their surface, which produces stronger repellent interaction among the nanoparticles and thus results in higher stability. As shown in Table III, all samples had negative zeta potential and S2 had the highest absolute value. Based on the results above, it was suggested that the nanoparticles had the highest encapsulation efficiency and stability when the drug content in feed was 10%.

Morphology

As shown in the TEM images [Fig. 3(a) and (b)], the blank and taxol-loaded MPEG-*b*-PCL nanoparticles were all spherical in shape with uniform size distribution, the diameters of which were all in the range of 20–25 nm. This further indicated that the taxol loading had no obvious effect on the size and shape of copolymer nanoparticles, which could be attributed to the low-drug loading. It could be found that the size of nanoparticle measured by TEM was smaller than that by DLS. The PEG chains on the nanoparticle surface are solvated and extended away from the particle surface in water; and the water molecules may go along with the particles during diffusion. These will all increase the particle size measured by DLS. The nanoparticles measured by TEM are in dry state, and the solvent drying leads to smaller sizes. Similar results had been reported: TEM images of the solid lipid nanoparticles showed that the diameters of nanoparticles were around 50 nm while the hydrodynamic diameter ranged from 124.67 to 156.67 nm as determined by PCS.[31] AFM image (Fig. 4) confirmed the narrow particle size distribution in a broader observing scope.

TABLE III
Drug Loading, Encapsulation Efficiency, Particle Size, and Zeta Potential of Taxol-Loaded MPEG-*b*-PCL Nanoparticles

Sample	D/C (%)	D.L. (%)	E.E. (%)	Hydrodynamic diameter (nm)	Polydispersity	Zeta potential (mV)
S1	5	1.86 ± 0.17	37.2 ± 3.4	90.4 ± 13.7	0.097	−5.20 ± 1.30
S2	10	5.25 ± 0.39	52.5 ± 3.9	87.1 ± 1.7	0.100	−12.22 ± 0.85
S3	15	5.62 ± 0.26	37.5 ± 2.6	98.8 ± 1.4	0.071	−6.56 ± 1.65
S4	20	5.26 ± 0.24	26.3 ± 1.2	75.4 ± 0.8	0.147	−7.87 ± 0.17

Values are expressed as average ± standard deviation ($n = 3$). D/C, feed ratio of drug to copolymer; D.L., drug loading of the nanoparticles; E.E., encapsulation efficiency of taxol. The hydrodynamic diameters were determined by DLS.

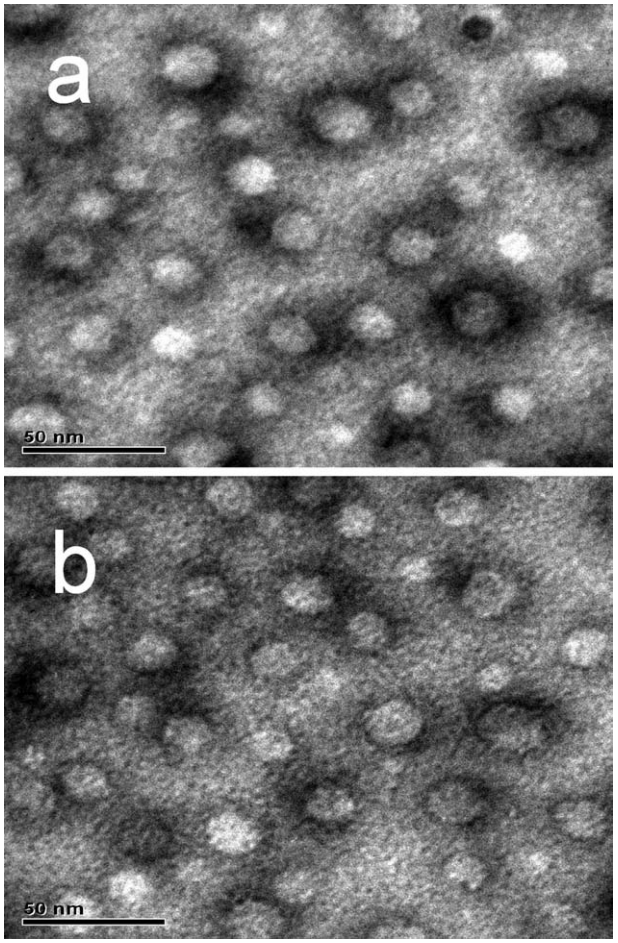

Figure 3 (a) TEM image of blank MPEG-*b*-PCL-1 nanoparticles; (b) TEM image of taxol-loaded MPEG-*b*-PCL-1 nanoparticles with drug loading 5.62% (S3 in Table III).

Stability

The change of particle size of taxol-loaded nanoparticles in ultrapure water with time at 4°C was investigated by DLS to evaluate the stability of nanoparticles. From Figure 5, it can be found that the average diameters of nanoparticles are in a range of 80–85 nm at all the time points, and the standard deviation values are in a range of 1.1–8.7 nm; thus, the particle sizes do not significantly vary for 15 days. The results suggested that disintegration or aggregation of nanoparticles in aqueous solution did not occur during the investigated period.

The stability of the nanoparticles in PBS 7.4 and FBS 7.4 was also evaluated. As shown in Figure 6(a), the hydrodynamic diameters did not vary significantly with time, and most of the error bars were short, indicating that the measured values of hydrodynamic diameter had good precision. Thus, it can be thought that the nanoparticles kept stable in either PBS 7.4 or FBS 7.4 for 24 h at 37°C. The result suggested that the nanoparticles were stable in biological media, and the biomolecules in FBS

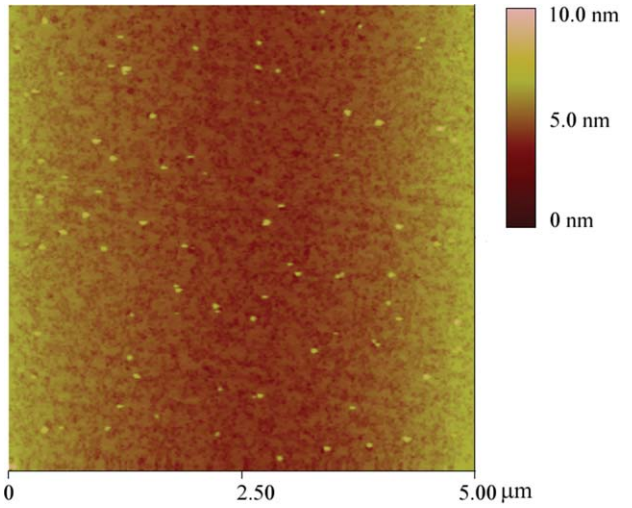

Figure 4 AFM image of taxol-loaded MPEG-*b*-PCL nanoparticles. [Color figure can be viewed in the online issue, which is available at wileyonlinelibrary.com.]

did not obviously interact with the nanoparticles. Figure 6(b) showed that the hydrodynamic diameters of the nanoparticles did not vary obviously in PBS 7.4 for 0 or 1 day at different concentrations of nanoparticles, ranging from 0.003% to 0.15% (w/v), most of the error bars were short. This suggested that the nanoparticles kept stable in PBS 7.4 at various concentrations of nanoparticles [0.003%–0.15% (w/v)].

In vitro release

The *in vitro* release profiles of taxol for the MPEG-*b*-PCL nanoparticles are shown in Figure 7. All nanoparticles with different drug loading (1.86–5.62%) released paclitaxel rapidly at the beginning

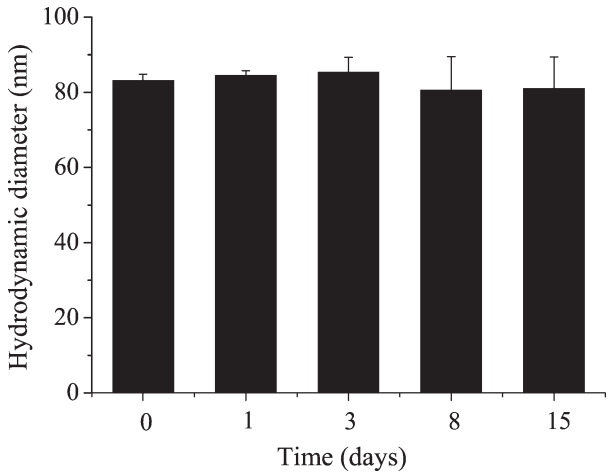

Figure 5 Hydrodynamic diameters versus time for the taxol-loaded MPEG-*b*-PCL nanoparticles in ultrapure water at 4°C. The diameters were measured by DLS, and the *y*-error bars represent standard deviation.

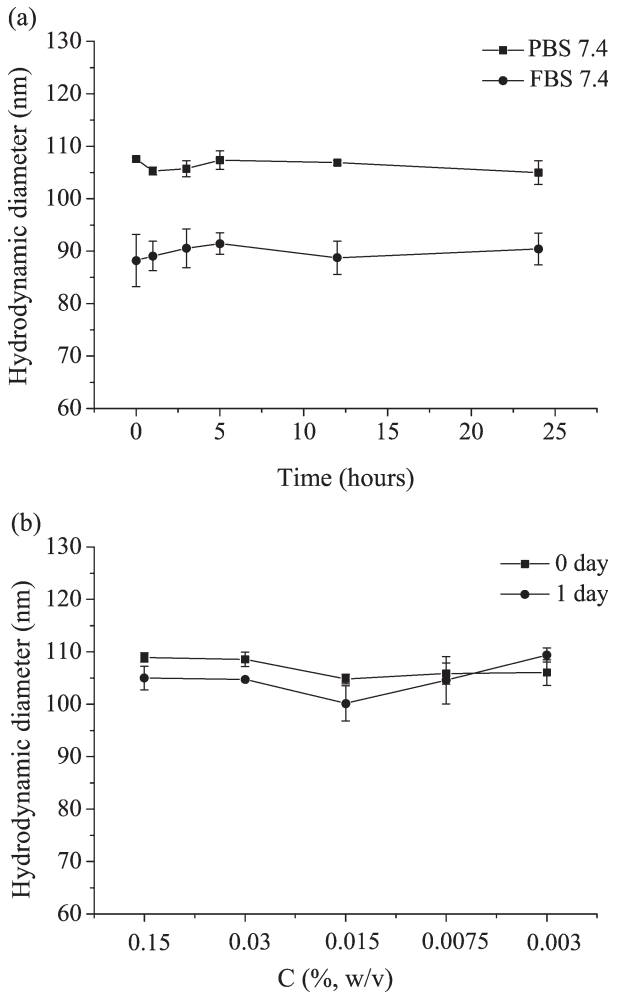

Figure 6 (a) Hydrodynamic diameters versus time for the taxol-loaded MPEG-*b*-PCL nanoparticles in PBS 7.4 and FBS 7.4 at 37°C, the values of *y*-error bars are in the range of 0.3–5.0 nm; (b) hydrodynamic diameters versus concentration of nanoparticles (c) for the taxol-loaded MPEG-*b*-PCL nanoparticles in PBS 7.4 at 37°C, the values of y-error bars are in the range of 0.2–4.5 nm. The diameters were measured by DLS ($n = 3$).

then slowly during the later period. The burst release of taxol might be ascribed to the fast dissolution of the drug located on the surface of the nanoparticles, while the slower and continuous release might be attributed to the diffusion of the drug encapsulated in the PCL core of the nanoparticles. The nanoparticles with drug loadings around 5% (S2, S3, and S4) could achieve a sustained release for 7 days. The release rate of taxol was dependent on the drug loading. The release rate of S1 with drug loading of 1.86% was distinctly faster than that of the nanoparticles with drug loadings around 5% (S2, S3, or S4). The cause might be that the drug presented as a molecular dispersion inside the nanoparticles at low,drug loading, while crystallization of drug occurred inside the nanoparticles at higher drug loading.[32,33] The crystallized drug could dissolve and

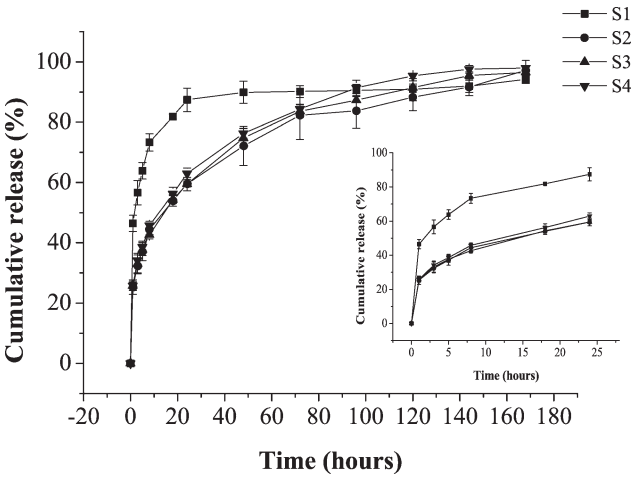

Figure 7 *In vitro* release profiles of taxol from the MPEG-*b*-PCL nanoparticles in 1% (w/v) Tween 80-PBS 7.4 at 37°C. Each data point represents the mean of triplicate samples. Most of the *y*-error bars are short, indicating small standard deviations and good precision.

diffuse more slowly into the outer aqueous phase than molecular dispersion.[15]

CONCLUSIONS

In this study, taxol-loaded MPEG-*b*-PCL nanoparticles were fabricated by solvent-evaporation method. Two kinds of MPEG-*b*-PCL with different PEG contents were applied as drug carrier and additive in the outer aqueous phase, respectively. We demonstrated that MPEG-*b*-PCL-2 with relatively high-PEG content could be a novel and very effective additive in the outer aqueous phase, resulting in high-encapsulation efficiency and excellent properties of taxol-loaded nanoparticles.

References

1. Wani, M. C.; Taylor, H. L.; Wall, M. E.; Coeggon, P.; McPhail, A.T. J Am Chem Soc 1971, 93, 2325.
2. Singla, A. K.; Grarg, A.; Aggarwal, D. Int J Pharm 2002, 235, 179.
3. Kongshaug, L.; Cheng, S.; Moan, J.; Rimington, C. Int J Biochem 1991, 23, 473.
4. Dorr, R. T. Ann Pharmacother 1994, 28, S11.
5. Tatou, E.; Mossiat, C.; Maupoil, V.; Gabrielle, F.; David, M.; Rochette, L. Pharmacology 1996, 52, 1.
6. Liggins, R. T.; Burt, H. M. Int J Pharm 2004, 282, 61.
7. Zhang, Z.; Feng, S. S. Biomaterials 2006, 27, 4025.
8. Yang, T.; Choi, M. K. J Control Release 2007, 120, 169.
9. Huh, K. M.; Min, H. S.; Lee, S. C.; Lee, H. J.; Kim, S.; Park, K. J Control Release 2008, 126, 122.
10. Soppimath, K. S.; Aminabhavi, T. M.; Kulkarni, A. R.; Rudzinski, W. E. J Control Release 2001, 70, 1.
11. Kim, S. Y.; Lee, Y. M. Biomaterials 2001, 22, 1697.
12. Mo, Y.; Lim, L. Y. J Control Release 2005, 108, 244.
13. Huang, C. Y.; Chen, C. M.; Lee, Y. D. Int J Pharm 2007, 338, 267.
14. Danhier, F.; Lecouturier, N.; Vroman, B.; Jérôme, C.; Marchand-Brynaert, J.; Feron, O.; Préat, V. J Control Release 2009, 133, 11.
15. Gref, R.; Minamitake, Y.; Peracchia, M. T.; Trubetskoy, V.; Torchilin, V.; Langer, R. Science 1994, 263, 1600.

16. Park, E. K.; Lee, S. B.; Lee, Y. M. Biomaterials 2005, 26, 1053.
17. Lu, Z.; Bei, J. Z.; Wang, S. G. J Control Release 1999, 61, 107.
18. Scholes, P. D.; Coombes, A. G.; Illum, L.; Davis, S. S.; Watts, J. F.; Ustariz, C.; Vert, M.; Davies, M. C. J Control Release 1999, 59, 261.
19. Feng, S. S.; Huang, G. F. J Control Release 2001, 71, 53.
20. Riess, G. Prog Polym Sci 2003, 28, 1107.
21. Mu, L.; Feng, S. S. J Control Release 2002, 80, 129.
22. Duncan, R.; Connors, T. A.; Meada, H. J Drug Target 1996, 3, 317.
23. Pascente, C.; Marquez, L.; Balsamo, V.; Muller, A. J. J Appl Polym Sci 2008, 109, 4089.
24. Youan, B.-B.C. J Appl Polym Sci 2006, 101, 1042.
25. Hou, J. W.; Guo, S. R. Acta Polym Sin 2009, 8, 796.
26. Sobczak, M.; Witkowska, E.; Oledzka, E.; Kolodziejski, W. Molecules 2008, 13, 96.
27. Cohn, D.; Stern, T.; Gonzalez, M. F.; Epstein, J. J Biomed Mater Res, Part A 2002, 59, 273.
28. Lu, C. F.; Guo, S. R.; Zhang, Y. Q.; Yin, M. Polym Int 2006, 55, 694.
29. Dong, Y. C.; Feng, S. S. Biomaterials 2005, 26, 6068.
30. Chansiri, G.; Lyons, R. T.; Patel, M. V.; Hem, S. L. J Pharm Sci 1999, 88, 454.
31. Xie, S. Y.; Wang, S. L.; Zhao, B. K.; Han, C.; Wang, M.; Zhou, W. Z. Colloid Surf B 2008, 67, 199.
32. Jeong, Y. I.; Cheon, J. B.; Kim, S. H.; Nah, J. W.; Lee, Y. M.; Sung, Y. K.; Akaike, T.; Cho, C. S. J Control Release 1998, 51, 169.
33. Jeong, Y. I.; Kang, M. K.; Sun, H. S.; Kang, S. S.; Kim, H. W.; Moon, K. S.; Lee, K. J.; Kim, S. H.; Jung, S. Int J Pharm 2004, 273, 95.